*Tectonophysics*, 77 (1981) 257—281
Elsevier Scientific Publishing Company, Amsterdam — Printed in The Netherlands



# STRUCTURAL STUDY OF THE ALMKLOVDALEN PERIDOTITE MASSIF (SOUTHERN NORWAY)

F. CORDELLIER [1], F. BOUDIER [1] and A.M. BOULLIER [2]

[1] *Laboratoire de Tectonophysique, Université de Nantes, 2 Chemin de la Houssinière, 44037 Nantes Cedex (France)*
[2] *Centre de Recherches Pétrographiques et Géochimiques, BP 682, 54037 Nancy Vandoeuvre (France)*

(Received June 26, 1980; revised version accepted January 12, 1981)

## ABSTRACT

Cordellier, F., Boudier, F. and Boullier, A.M., 1981. Structural study of the Almklovdalen peridotite massif (southern Norway). Tectonophysics, 77: 257—281.

The Almklovdalen ultramafic body included in the basal gneisses of southern Norway is composed mainly of hydrated harzburgite and dunite with cores of layered garnet lherzolite. From field and gravity evidence, the body can be interpreted as a deformed cone surrounding a gneiss central mass. Based on structural, microstructural and mineral preferred orientation (MPO) studies a continuous kinematic and metamorphic history is inferred. The major events of this history starting 1400—1800 million years ago are:

(1) Intrusion of a garnet-bearing peridotite slice from mantle into crust and folding of garnet-rich $S_0$ layers inducing an $S_1$ foliation and an $L_1$ lineation marked by flattening and elongation of garnet and olivine crystals. Traces of high-temperature slip in olivine porphyroclasts are found. Strong annealing had a scattering effect on MPO.

(2) Pervasive deformation in the peridotites and in the surrounding gneisses coinciding with introduction of water in the peridotites. It is responsible for isoclinal folding with $S_2$ foliation and $L_2$ lineation marked by chlorite and amphibole flattening and elongation in the peridotites.

(3) Gravity sinking of the whole slice in the acidic gneisses of the crust creating a cup-like shape. This event is responsible for an $S_3$ foliation marked by chlorite flattening parallel to the peridotite—gneiss contact and for an $L_3$ lineation, marked by chlorite elongation and spinel strings, parallel to the generatrix of the imperfect cone. MPO's of the peridotite indicate slip in olivine following different systems. Enlargement of olivine porphyroblasts occurs due to annealing. The gravity sinking is contemporaneous with the almandine amphibolite metamorphism in the gneiss where it develops a foliation and lineation parallel to those in the peridotites.

(4) Deformation possibly due to a north—south compression which induces an $S_4$ foliation and $L_4$ lineation in the gneiss, parallel to the axial planes and the axes of the two folds affecting the peridotite body.

## INTRODUCTION

Considerable interest has been devoted to garnet peridotites since results of experimental petrology have pointed out that their conditions of equilib-

0040-1951/81/0000—0000/$02.50 

rium correspond to those of the deepest samples of the upper mantle (O'Hara and Mercy, 1963). Garnet peridotites are observed in two kinds of occurrences: (1) as xenoliths in kimberlites from stable continental areas; (2) as small massifs or bodies scattered in the basement rocks of continental regions which have suffered later orogeneses (Czechoslovakia, Austria, Switzerland, Massif Central of France, Norway).

Some authors, e.g., O'Hara and Mercy (1963), Carswell (1968, 1973), Lappin (1974), Carswell and Gibb (1980), Medaris (1980), have thought that these massifs represent slices of the subcontinental upper mantle, emplaced in early episodes of crustal history. Other authors like Bryhni et al. (1970), Rost et al. (1974), Tromsdorf and Evans (1974) preferred a secondary origin for the garnet in these peridotites. Thus, the possibility of a mantle origin for garnet with preservation of mantle parageneses and textures is questioned. Garnet-peridotite bodies have already been investigated structurally and texturally by Lappin (1966, 1967) for the Almklovdalen massif and by Möckel (1969) for the Alpe Arami massif in the Swiss Alps. Möckel described preferred orientations (MPO) of olivine which are very different from those of other investigated mantle peridotites (review in Nicolas and Poirier, 1976), whereas Lappin observed a diffuse and somewhat variable MPO of a type commonly found for olivine.

The aim of this paper is to investigate the sequence of tectonic events in the peridotite bodies and surrounding gneiss by carrying out a field study and by detailed structural and textural analyses to gain insight of the deformation history since the possible emplacement of the bodies from the mantle into the crust.

## THE ALMKLOVDALEN PERIDOTITE

In the Nordfjord region, scattered ultramafic bodies are aligned E—W to NE—SW, following the foliation in the gneiss (Bryhni, 1966).

The Almklovdalen peridotite body crops out on the northern side of the Nordfjord (Fig. 1). It belongs to a series of ultramafic bodies included in the Fjordan unit of the basal gneiss region. This complex of western Norway is considered to be polymetamorphic and polygenetic. The ultramafic lenses have possibly undergone three orogenic events: the Svecofennian cycle (1600—1800 Ma), the Sveconorvegian cycle (900—1200 Ma), and the Caledonian cycle (350—600 Ma) (Brueckner, 1975). Indeed, ages as old as 1800 Ma have been reported by Mc Dougall and Green (1964) in eclogites; they are confirmed by Brueckner (1972), Pidgeon and Raheim (1972), Mysen and Heier (1972) and Jacobsen (1980) in almandine-amphibolite facies gneisses which enclose the ultramafic bodies. $^{87}Sr/^{86}Sr$ ages of the Caledonian cycle are reported by Brueckner (1975) from a fracture-vein dunitic assemblage in the Almklovdalen peridotite, and numerous K/Ar dates in the range of 372—590 Ma (Bryhni et al., 1970) suggest the influence of a Caledonian event in the Fjordan complex, accompanied by reequilibration in the lower amphibolite facies.

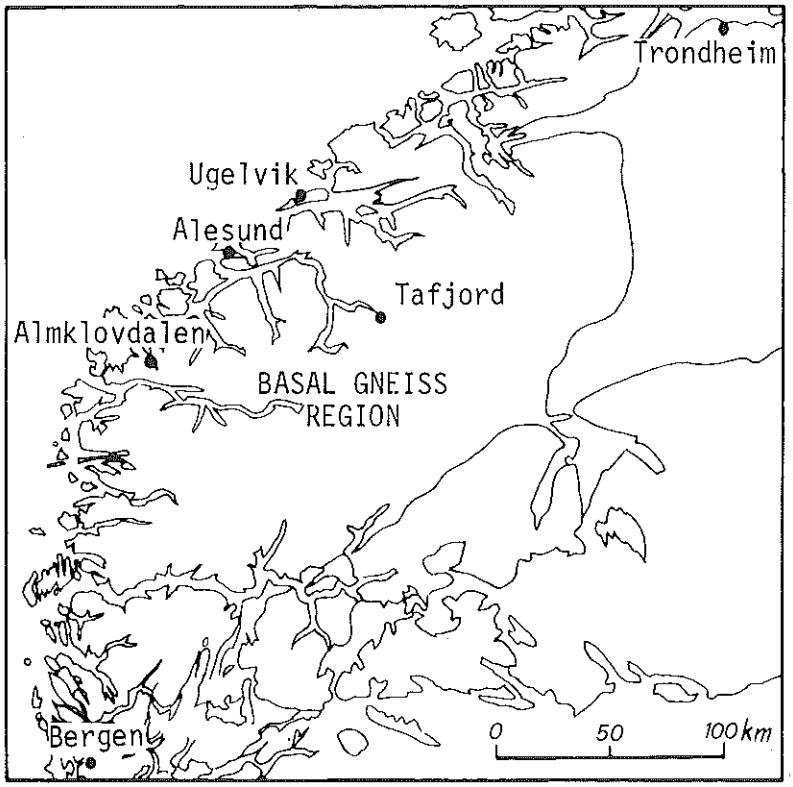


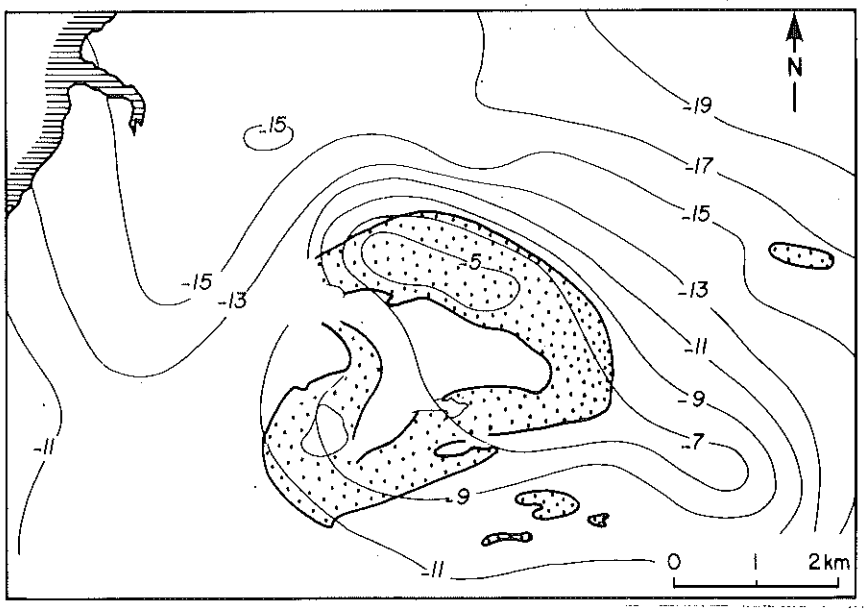


Fig. 1. Simplified geologic map of the Almklovdalen area and Bouguer gravity anomaly contours in milligals (from Grønlie and Rost, 1974). Dots = ultramafic bodies, undecorated area = basal gneiss complex.

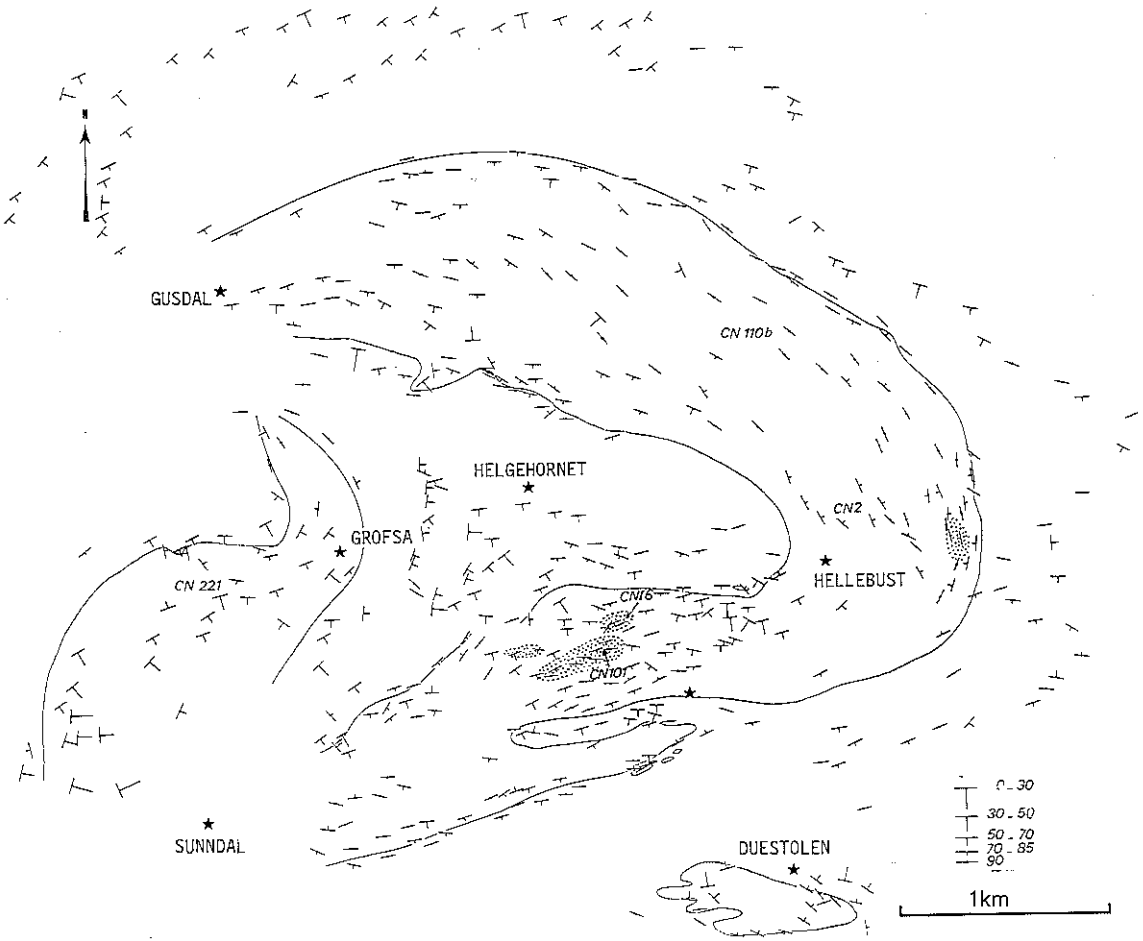


Fig. 2. Map of foliations in the peridotite, in the central gneiss mass of the Helgehornet, and in the surrounding gneiss. Dotted areas are outcrops of garnet peridotite. Full contours correspond to observed contacts between peridotite and gneiss. Numbers are sample numbers.

The general shape of the Almklovdalen peridotite is uncertain, due to poor outcrop in the zones of Gusdal, Hellebust, and Sunndal. Lappin (1966) mapped three different bodies; on the basis of gravity data Grønlie and Rost (1974) suggested that the ultramafic body extended towards the southeast under the surrounding gneiss (Fig. 1). The orientation of the mesoscopic structures in the peridotites and in their country rocks indicates that the megascopic structure consists of two asymmetric folds, nestled within each other: the Gusdal-Hellebust-Sunndal fold to the east, and the Gusdal-Grofsa-Sunndal folds to the west (Fig. 2). The characters of these folds will be analysed in more detail in the following section.

## PARAGENESES AND STRUCTURAL ELEMENTS

Structural elements are defined in relation to parageneses. Three petrographic facies are represented in the Almklovdalen peridotite: garnet lherzolite, chlorite harzburgite, and dunite. The garnet peridotite occurs inside the eastern peridotite fold, near Lia, as lenses a few hundred meters long, bounded by subvertical shear zones, and near Hellebust as one small mass bounded by shear zones (Figs. 2 and 3). Because of their occurrence inside the chlorite harzburgites and dunites, the garnet peridotites appear to be preserved relict masses. There is no evidence of any systematic arrangement of harzburgites and dunites in the peridotite body.

### *Garnet-peridotite and garnet-pyroxenite banding*

Remarkably fresh garnet peridotite is observed in the Almklovdalen massif. The paragenesis is olivine + orthopyroxene + clinopyroxene + garnet + accessory spinel. Pargasitic amphibole develops in the vicinity of garnet crystals into aggregates parallel to the foliation. The foliation ($S_1$) is marked by flattening of olivine crystals and of garnets. With the garnet peridotite occur garnet-pyroxenite bands. The garnet-pyroxenite banding (Fig. 4B) has a maximum thickness of 40 cm with diffuse boundaries; it is composed of the same minerals as the enclosing peridotite although in a different ratio. The characters are typical of type I primary banding in lherzolites (Boudier, 1976). In this regard it is similar to the garnet-pyroxenite banding of Alpe Arami (Möckel, 1969), but is different from type II garnet-pyroxenite banding of Lherz (southern France), Ronda (southern Spain) and Beni Bouchera (Morocco) massifs because it is not recrystallized. Parallel bands are commonly observed in peridotite massifs and in xenoliths from basalt and kimberlite. Their occurrence in xenoliths demonstrates their possible mantle origin. The foliation is generally discordant with the garnet-pyroxene banding ($S_0$) and paralel in general, to the axial plane of folds affecting the banding (Fig. 4A and 4B). A lineation ($L_1$) is marked by unaltered and slightly elongated garnets. It is parallel to $S_0/S_1$ intersection.

In the shear zones bounding the garnet-peridotite cores, the paragenesis

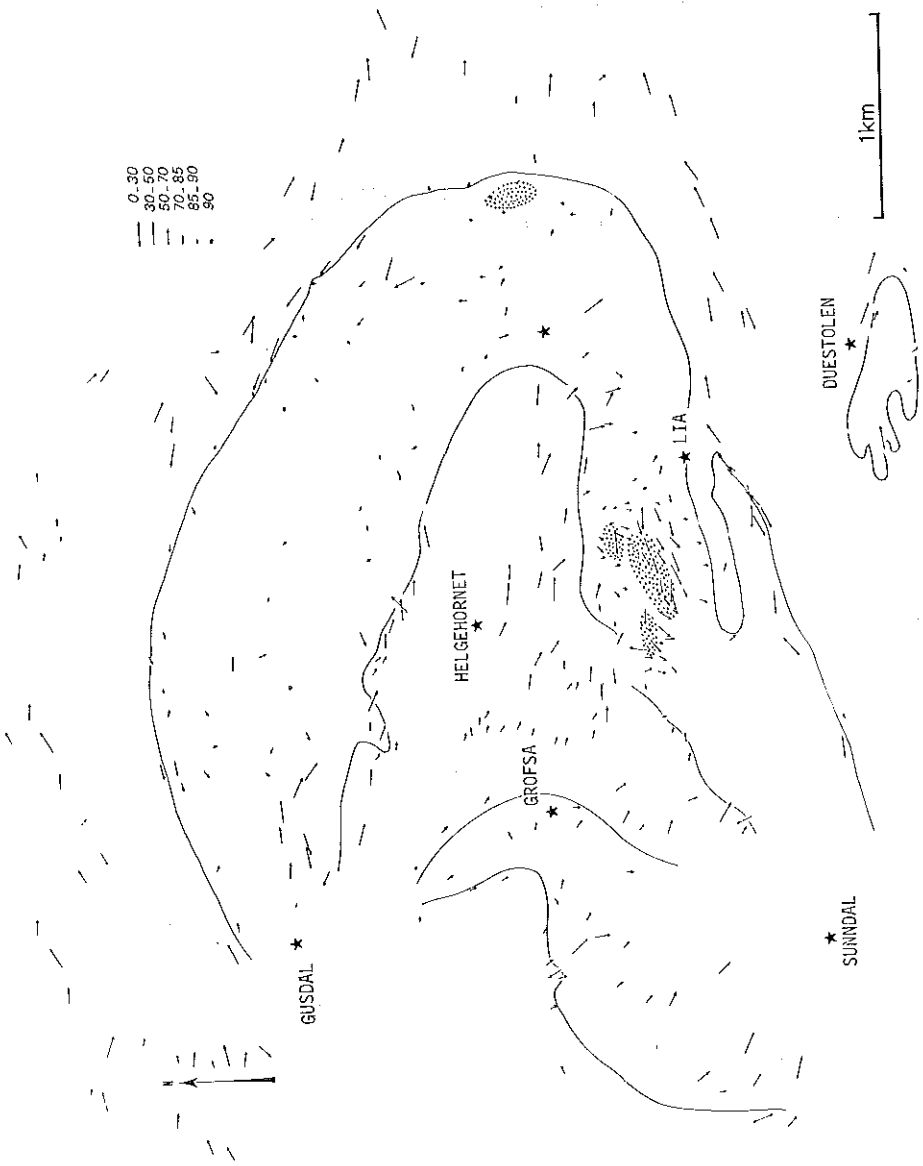


Fig. 3. Map of lineations in the peridotite and gneiss.

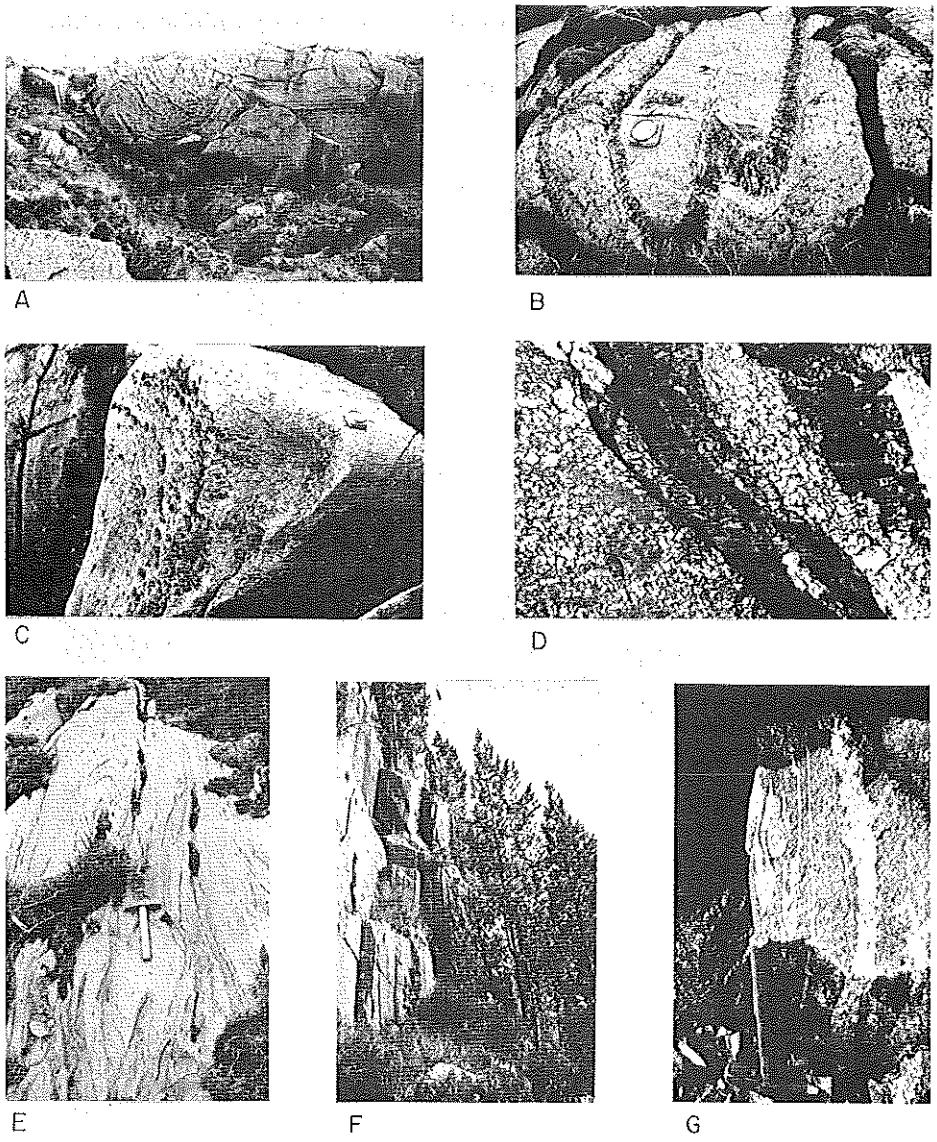


Fig. 4. A. $D_1$ deformation producing a parallel fold, overturned to the north, in garnet peridotite layers ($S_0$) from the garnet-peridotite body near Lia.
B. Same deformation in garnet peridotite, the subvertical foliation $S_1$ with flattened garnet lies in the axial plane of the fold.
C. $D_2$ deformation in chlorite-peridotite of the shear zone. The subvertical $S_2$ foliation (flattening of chlorite) is the axial plane of $S_0$ folds. $L_2$ lineation is parallel to the fold axis.
D. $D_3$ deformation in the central gneiss body; quartz-feldspar rods are parallel to $L_3'$.
E. $D_2$ deformation: isoclinal folding with vertical axis in chlorite-peridotite bounding the Lia garnet-peridotite body.
F. $D_3$ deformation: tectonic banding in chloritized dunite close to the contact with gneiss.
G. $D_4$ deformation: isoclinal folding in the surrounding gneiss.

changes by a rapid transformation of the garnet into amphibole + chlorite aggregates (Fig. 4C). These aggregates are strongly elongated in a new foliation plane, also defined by the flattening of olivine and called $S_2$. Keliphitic rims around garnet have formed after the transformation into amphibole +

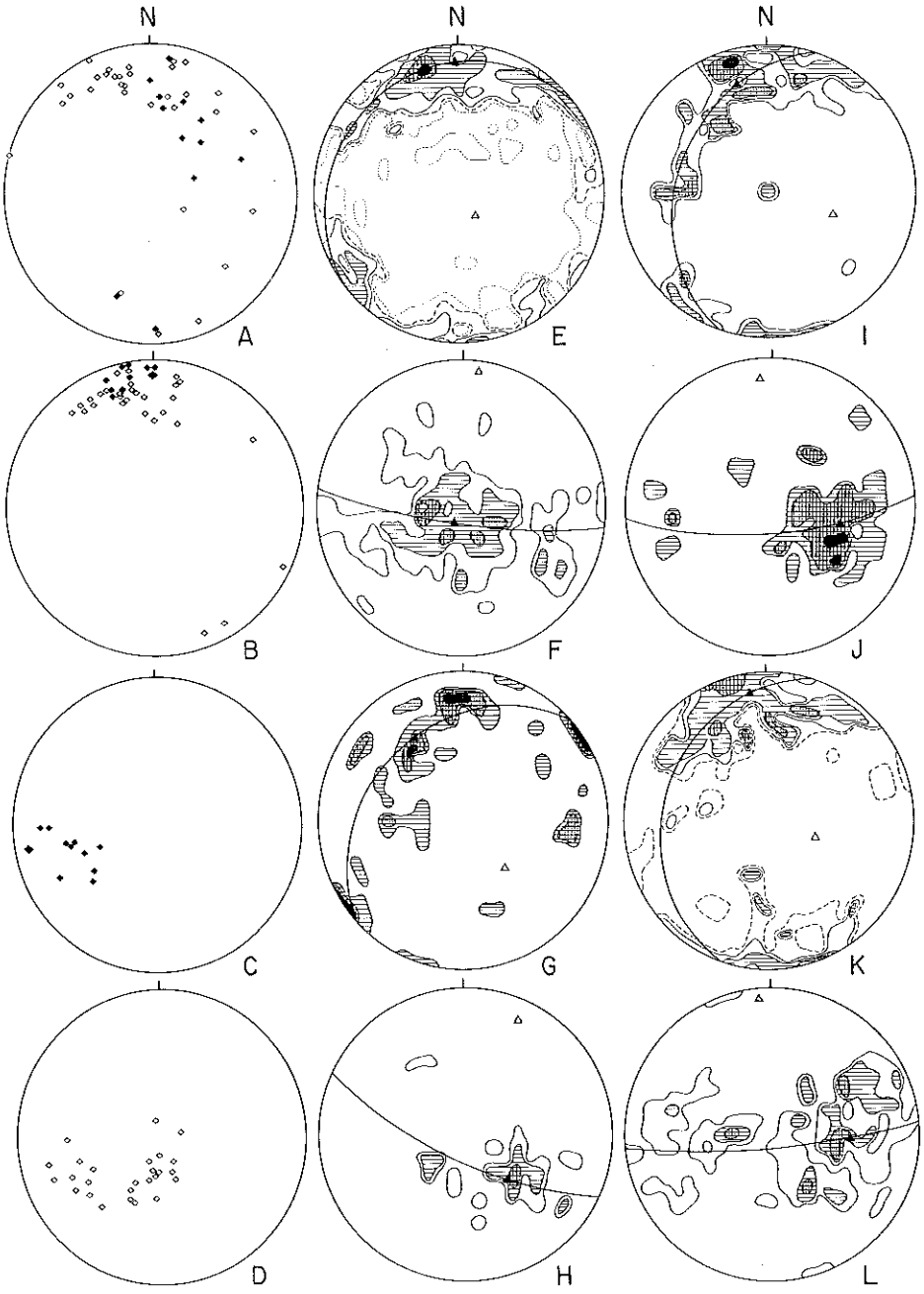

chlorite. A lineation ($L_2$) associated with $S_2$ is marked both by elongation of chlorite aggregates and olivine crystals and by the intersection between $S_2$ and the chloritized and laminated banding $S_0$, folded isoclinally (Fig. 4E).

In the garnet-peridotite lenses near Lia, foliations in the unaltered garnet peridotite ($S_1$) and in the chloritized garnet-peridotite ($S_2$) are parallel, chlorite and amphibole growing parallel to the garnet flattening; they strike E—W, and dip steeply to the south (Fig. 5B). The lineations ($L_1$), marked by unaltered and slightly elongated garnet, and ($L_2$) marked by chloritized garnets, trend E—W, and plunge 10—40° to the west (Fig. 5C): the garnet-pyroxenite banding $S_0$ in the garnet peridotite is deformed into parallel folds $F_1$ overturned to the North (Figs. 4A, B and 5A). The foliations ($S_1$, $S_2$) and the lineations ($L_1$, $L_2$) are parallel to axial planes and axes of these folds respectively (Fig. 5A—C).

In the amphibole + chlorite-bearing peridotite of the shear zones surrounding the garnet-peridotite cores, the foliation $S_2$ has the same orientation as in the garnet peridotite (Fig. 5B), but the lineation $L_2$ shown by amphibole + chlorite aggregates steepens progressively from gently plunging to the west, to subvertical to the east (Fig. 5D). During deformation which formed $S_2$ and $L_2$, isoclinal folds developed (Fig. 4E) with fold axes $F_2$ plunging W55° to 90° and parallel to the $L_2$ lineation and $S_2$ foliation parallel to the axial plane. $F_2$ folds do not refold $L_1$. The chloritized pyroxenitic banding $S_0$ rotates abruptly into parallelism with the $S_2$ foliation, so that the olivine—chlorite banding in the shear zone can be interpreted as a transposition of the original banding $S_0$.

---

Fig. 5. Lower hemisphere equal area projection of field structures.
A. Poles to garnet-pyroxenite banding $S_0$ in the garnet-peridotite body near Lia. Solid lozenges represent fresh garnet banding; open lozenges, chloritized garnet banding.
B. Poles to foliations $S_1$ marked by flattening of fresh garnet (solid lozenges), $S_2$ marked by chloritized garnet (open lozenges) in the garnet-peridotite body near Lia.
C. Same areas as A and B: garnet lineation $L_1$.
D. Same areas as A and B: chloritized garnet lineation $L_2$.
E and G. Poles to foliation $S_3$ in the chlorite peridotite. E. Eastern fold, 345 measurements, contours: 0.25, 0.5, 1, 2, 4, 8%. G. Western fold, 41 measurements, contours 2, 4, 8% per 0.45% area.
F and H. Lineation $L_3$ in the chlorite peridotite. F. Eastern fold, 149 measurements, contours: 1, 2, 4, 8%. H. Western fold, 28 measurements, contours: 4, 8, 16% per 0.45% area.
I. Poles to foliations $S_3'$ and $S_4$ in the central gneiss body, 83 measurements, contours: 1, 2, 4, 8% per 0.45% area.
J. Lineations $L_3'$ and $L_4$ in the central gneiss body, 64 measurements, contours: 2, 4, 8% per 0.45% area.
K. Poles to foliation $S_4$ in the surrounding gneiss, 177 measurements, contours: 0.5, 1, 2, 4, 8% per 0.45% area.
L. Lineations $L_4$ in the surrounding gneiss, 100 measurements, contours: 1, 2, 4, 8% per 0.45% area.
Triangles indicate the computed point maxima and pole maxima.

The structures analysed in the garnet-peridotite cores and adjacent chlorite-peridotite shear zones suggest two possible interpretations: either they represent two independent deformations — the one associated with chloritization having coincidentally a similar geometry as the one imprinted in the garnet-peridotite facies, or there is a continuum of deformation starting in the garnet-peridotite facies and evolving during chloritization of garnet. Finally, as the deformation concentrates in shear zones during increasing chloritization of the peridotites, the axial plane of folds remains unchanged but the plunge of fold axis increases westward. The second interpretation is preferred because of the continuity suggested by the analyses of both the structures and parageneses.

*Chlorite peridotite*

Chlorite peridotite represents transitions from chlorite harzburgite to chlorite dunite. Amphibole is present in harzburgites, but absent in dunites. All facies contain a black spinel dispersed in the olivine matrix. Chlorite is present in variable amounts. Chlorite lamellae occur generally at olivine grain boundaries and sometimes as inclusions in large olivine porphyroblasts (see p. 276). A new foliation ($S_3$) is defined by flattened olivine and the orientation of chlorite lamellae. Also a new lineation ($L_3$) develops marked by the elongation of chlorite lamellae, and by the spinel strings. $S_3$ foliation never intersects $S_2$.

Chlorite peridotites are constituant of the major part of eastern and western bodies. The geometry of the deformation is slightly different in the two bodies in that the $S_3$ foliation dips more gently in the western body. In both bodies, the foliation $S_3$ (Fig. 4F) is folded together with the peridotite—gneiss contact (Figs. 2, 5E, G). The axial plane of these folds $F_3$ is defined as $S_4$ and is parallel to the general E—W subvertical attitude of the foliation in the gneisses; the mineral lineation $L_3$ tends to parallel to the fold axes (Fig. 5E—H). The average plunge is 80° to the SE for the axis of the eastern fold (Fig. 5E), and 65° to the SE for the axis of the western fold (Fig. 5G). $F_3$ does not refold $L_2$ neither $L_1$.

*Gneisses*

Gneisses show a retrograde evolution from almandine-amphibolite facies to epidote-amphibolite facies. Relicts of almandine-amphibolite facies are restricted to the western part of the Helgehornet body. In these facies the foliation, defined as $S_3'$, is parallel to the contact with peridotite. In the retrograde epidote-amphibolite gneiss of other places the foliation is defined as $S_4$. The associated lineations $L_3'$ (Fig. 4D) and $L_4$ are both mineral lineations (elongation of quartz + feldspar aggregates).

Gneisses crop out inside the peridotite mass (Helgehornet body) and in the surrounding domain. The metamorphic layering and ($S_4$) foliation (Fig.

4G), defined by biotite and amphibole flattening, show an E—W trend and a subvertical dip (Fig. 5K) except in the western part of the Helgehornet body where an older layering $S_3'$ is folded along with the western peridotite body contact (Figs. 2 and 6). Small-scale folds of $S_3'$ with $S_4$ as axial plane are produced in this hinge area. The E—W striking $S_4$ foliation is parallel to the axial plane of the large-scale folds of $S_3'$ in the gneiss, of $S_3$ in the peridotite, and of the contact gneiss—peridotite.

The $L_3'$ lineation constitutes the dominant structural elements in the fold hinge of the western Helgehornet (Fig. 4D) where it typically has the character of a stretching lineation.

The mineral lineation $L_4$ tends to be parallel to the fold axes in the gneiss and to the intersection of $S_3'/S_4$ in the western part of the Helgehornet body. The $L_4$ mineral lineation in the other gneiss occurrences has the same orientation (Fig. 5J, L).

Consequently, the large-scale folding of the two peridotite bodies and of the Helgehornet gneiss is interpreted as formed by a dominant compressional phase of deformation during a flow which is responsible for the $L_4$ lineation. This phase would slightly postdate the development of the foliation $S_3'$ and lineation $L_3'$ in the gneiss and the almandine-amphibolite facies metamorphism.

## CHRONOLOGY OF DEFORMATIONS

The proposed chronology is presented in Table I and Fig. 6, and is based on the relationship of deformation episodes with metamorphic transformations in the peridotite. Following the evidence that amphibole and chlorite developed after garnet, the equilibrium of the peridotite in the amphibolite-chlorite facies postdates the achievement of equilibrium in the garnet facies. The garnet-peridotite lenses represent the oldest preserved facies, implying also an old origin for the deformation ($D_1$) imprinted in the garnet peridotite with garnet flattening and elongation ($S_1$, $L_1$) and parallel folding of the pyroxenitic banding $S_0$. In this $D_1$ deformation the axial plane strikes E—W and dips steeply to the south and the fold axes are gently plunging to the west. The physical conditions of equilibrium in the garnet-peridotite facies would be $P = 12$—$15$ kb, $T \simeq 850°$C (O'Hara et al., 1971), or $P = 20.7$ — $23.1$ kb, $T \simeq 750°$C (Carswell and Gibb, 1980); more recent data by Medaris (1980) indicate ranging pressure $17\text{ kb} < P < 28\text{ kb}$ and temperature $545°\text{C} < T < 820°\text{C}$ for the Almklovdalen garnet peridotite.

This $D_1$ deformation evolves into a $D_2$ deformation during chloritization of garnet, geometrically accompanied by an increasing plunge to the west of the mineral lineation and fold axes; the $S_2$ foliation has also an E—W strike and dips steeply to the south. The $D_2$ deformation generated shear zones bounding the garnet peridotite lenses. Temperatures and pressures during $D_2$ were on the boundary of the garnet peridotite and chlorite peridotite facies: $P \simeq 10$ kb, $T \simeq 700°$C (Rost, 1971).

TABLE I

Deformation path in the Almklovdalen body

| Area | Paragenesis associated with deformation | Association | Location and style of the deformation | Domain of equilibrium | $P/T$ conditions | Deformation phases |
|---|---|---|---|---|---|---|
| Garnet-peridotite bodies | $S_0$ = pyroxenitic primary banding<br>$S_1$ = garnet<br>$L_1$ = garnet | $S_1$ = S80<br>$L_1$ = W10—40 | $F_1$, open folds in garnet peridotite | garnet peridotite | $P$ = 12—15 Kb<br>$T < 850°$ C<br>(O'Hara et al., 1971)<br>$P$ = 17—28 Kb<br>$T$ = 645—820° C<br>(Medaris, 1980) | $D_1$ |
| Chlorite-amphibole-bearing garnet peridotite | $S_2$ = chloritized garnet<br>$L_2$ = chloritized garnet | $S_2$ = S80<br>$L_2$ = W20—80 | $F_2$, intrafolial folds in chlorite peridotite (shear folding) | boundary of garnet peridotite: chlorite peridotite | $P$ = 12—15 Kb<br>$T < 850°$ C<br>(O'Hara et al., 1971)<br>$P \sim$ 10 Kb<br>$T \sim 700°$ C<br>(Rost, 1971) | $D_2$ |
| Eastern and western peridotite bodies | $S_3$ = chlorite lamellae in the peridotite<br>$L_3$ = chlorite lamellae, spinel elongation | $S_3$ = rotated with $L_3$ fold axis<br>$L_3$ = SE80 eastern fold, SE40 western fold | $F_3$, parallel folding in chlorite peridotite, large-scale folding of eastern and western peridotite bodies, with $S_3$ as axial plane | chlorite peridotite | $P < 10$ Kb<br>$T < 700°$ C<br>(Rost, 1971)<br>$P \sim 7$ Kb<br>$T$ = 650—700° C<br>(O'Hara et al., 1971) | $D_3$ |
| Central gneiss | $S_3'$ = biotite in garnet gneiss<br>$L_3'$ = amphibole, quartz feldspar aggregates | $S_3'$ = rotated with $L_3'$ as fold axis<br>$L_3'$ = E40 | $F_3'$ intrafolial folds and large-scale folding in the gneiss with $S_3$ as axial plane | almandine-amphibolite facies | $P \sim 7$ Kb<br>$T$ = 650—700° C | |
| Central and surrounding gneiss | $S_4$ = biotite in biotite gneiss<br>$L_4$ = amphibole biotite | $S_4$ = S80<br>$L_4$ = E40 | dominant flattening component | biotite-amphibolite facies | | $D_4$ |

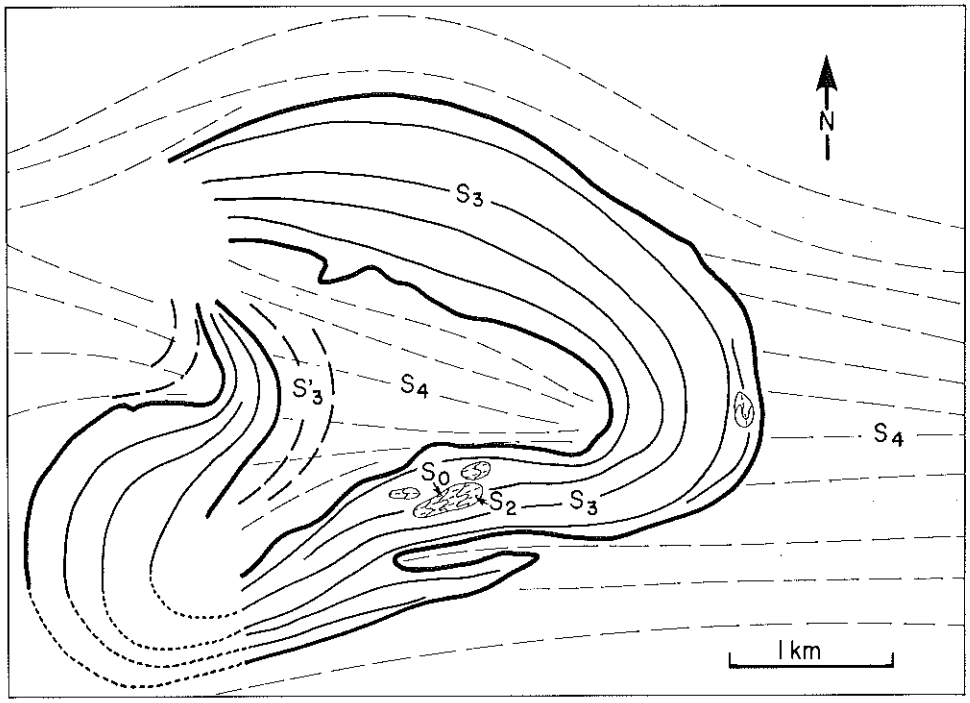


Fig. 6. Interpretative structural map of the Almklovdalen body. Interpolated contours are dashed.

Deformation $D_3$ is related to the development of $S_3$ foliation in the whole peridotite mass. The $S_3$ foliation is subvertical and mainly E—W striking. The mineral lineation $L_3$ is subvertical to E50 in the eastern peridotite body and plunges moderately to the SE in the western peridotite body. The development of foliation and metamorphic layering in the gneiss is also attributed to $D_3$ since the foliation $S'_3$ in it, is parallel to the foliation $S_3$ in the chlorite peridotite and the equilibrium conditions of the almandine-amphibolite facies in the gneiss ($P = 7$ kb and $T \simeq 650°—700°$ C) are in the same range as those fixed by the chlorite-peridotite equilibrium.

The last identified deformation ($D_4$) is geometrically related to the large folding of the Almklovdalen body. It may be responsible for this folding or possibly the modification of the geometry of a previous fold. This folding deforms the $S_3$ foliation of chlorite peridotites and $S'_3$ foliation defined in the surrounding and eastern central gneiss. The foliation $S_4$ strikes E—W. The horizontal trend of the lineation $L_4$ in the surrounding gneiss (Fig. 3 and Bryhni et al., 1966) and its tendency to increasing plunge like that of the fold axes in the vicinity of the peridotite body, would suggest that $D_4$ was essentially due to a N—S oriented compression, accompanied by an E—W flow (Nicolas and Boudier, 1975) locally perturbed by the presence of a competent peridotite body.

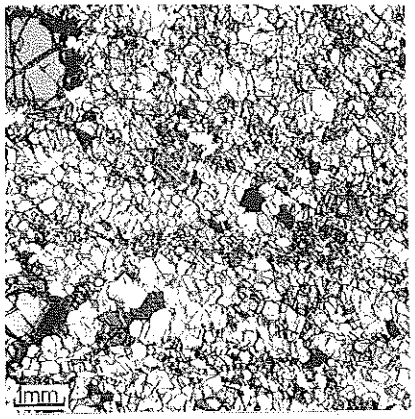


A

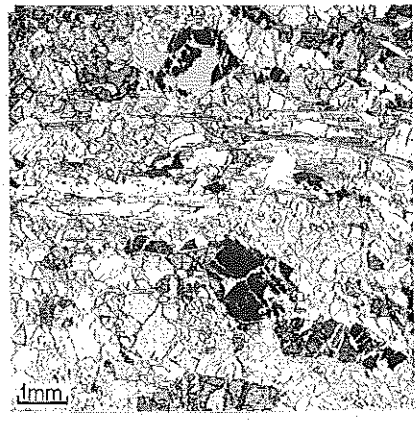


B

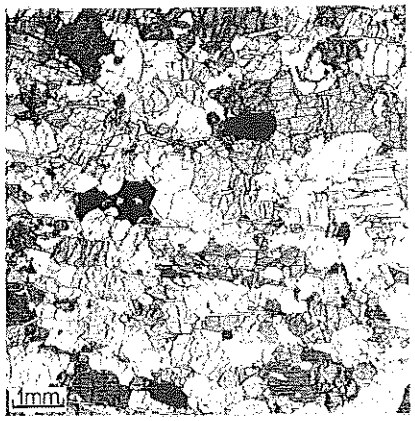


C

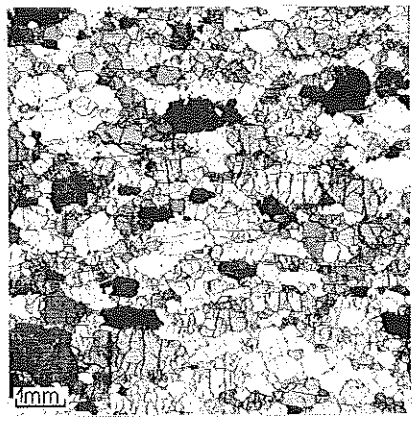


D


E

Two main points are drawn from this analysis:

(a) The geometrical coincidence of the successive foliations $S_1, S_2, S_3, S'_3$, $S_4$ is probably due to a reorientation of previous structures during $D_4$ deformation. The preservation of the attitudes of the older lineations $L_1$, $L_2$, $L_3$, $L'_3$, emphasizes the dominant compressional character of $D_4$.

(b) Although the appearance of a four stage deformational sequence is derived from the structural analysis, the study of the peridotite suggests a continuous deformation path, the deformation being accompanied by introduction of water and evolving under retrograde $P$—$T$ conditions from the garnet-peridotite facies to the amphibolite facies.

## TEXTURES AND MINERAL PREFERRED ORIENTATION

Textures in Almklovdalen peridotites are previously characterized by a strong annealing with abundant development of neoblasts devoid of substructure (Lappin, 1967). Textures of peridotites in the Almklovdalen peridotites are here described as transitional between three main types: mosaic equigranular, mosaic tabular (Boullier and Nicolas, 1975), and porphyroblastic.

### *Mosaic equigranular texture* (Fig. 7A)

The mosaic equigranular texture characterizes the garnet peridotite. Polygonal olivine neoblasts (0.2—0.5 mm) have a weak mineral preferred orientation (MPO). Enstatite neoblasts form, in association with finer grain-sized (0.1—0.3 mm) olivine, bands parallel to the foliation. Porphyroclasts (2—5 mm) of olivine, orthopyroxene and clinopyroxene represent approximately 10% in volume. Olivine porphyroclasts exhibit a $(100)_{ol}$ substructure oblique to the trace of the foliation in this section. Garnet is present as slightly elongated porphyroclasts (2—8 mm) surrounded by pargasitic amphibole and chlorite (0.2—0.5 mm) growing in the foliation plane. The corresponding MPO's are presented in Fig. 8A. Crystallographic axes of olivine neoblasts show no preferred orientation. The enstatite makes a poorly defined $[001]_{en}$ girdle slightly oblique to the foliation.

---

Fig. 7. Textures in peridotites in thin sections perpendicular to the foliation and parallel to the stretching lineation (E—W).

A. Equigranular mosaic texture in garnet peridotite from Lia body. Specimen CN 16, MPO in Fig. 8A.

B and C. Transitions from equigranular mosaic to equigranular tabular texture in chlorite harzburgite. B. Specimen CN 101, from shear zones near Lia body, MPO in Fig. 8B. C. Specimen CN 170 b, from Eastern fold, MPO in Fig. 8C.

D. Equigranular tabular texture in dunite. Specimen CN 221, from the western fold, MPO in Fig. 8D.

E. Porphyroclastic texture in chlorite harzburgite. Specimen CN 2, from the Eastern fold MPO in Fig. 8E.

This texture is interpreted as being derived from a coarser texture whose grain size is given by the relict porphyroclasts (2—5 mm). The deformation appears to have taken place at high temperature conditions as indicated by the dominant high temperature $[100]_{ol}$ slip direction (Nicolas and Poirier, 1976) deduced from the occurrence of $(100)_{ol}$ sub-boundaries in olivine porphyroclasts (Fig. 7A). The size, the shape of olivine neoblasts, and the slight misorientation between adjacent neoblasts suggest a mechanism of recrystal-

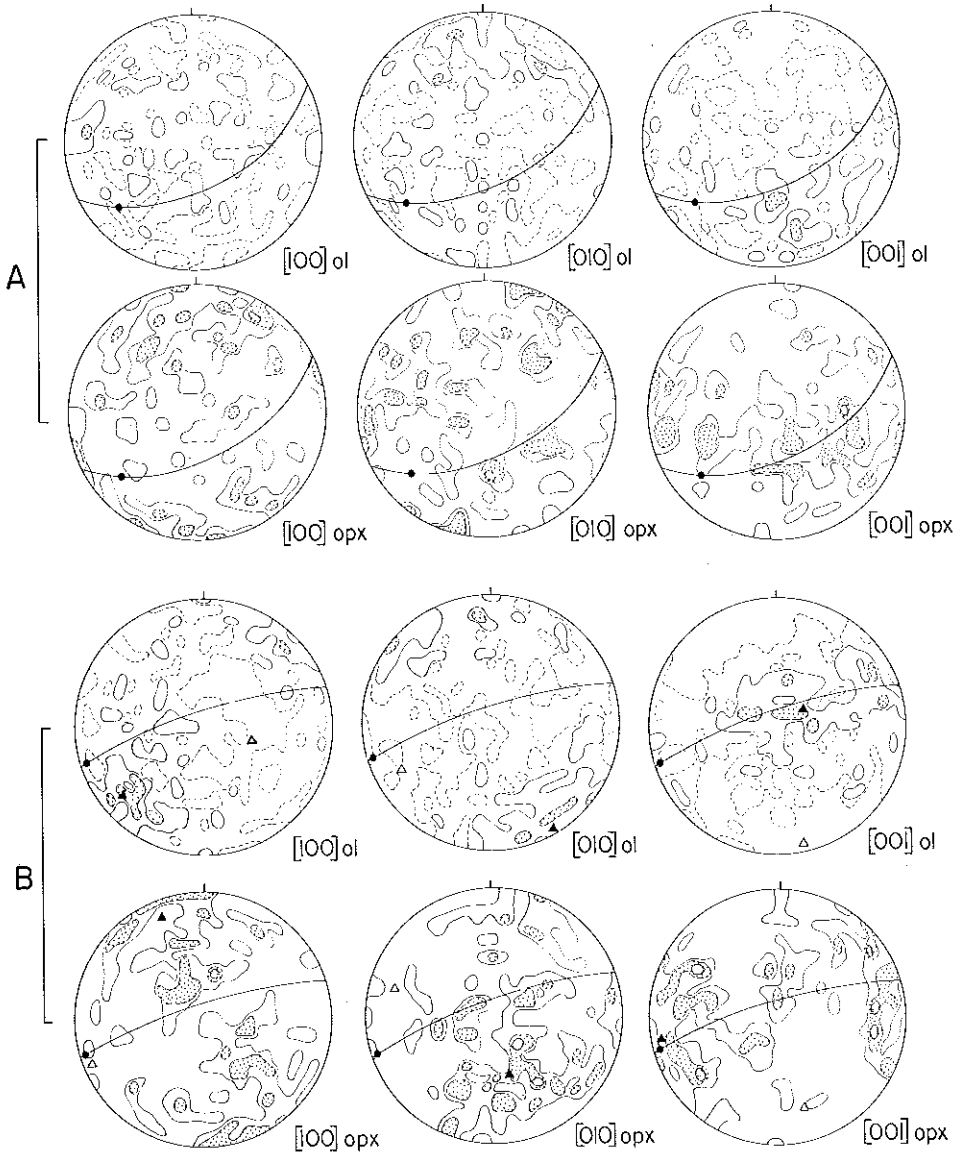

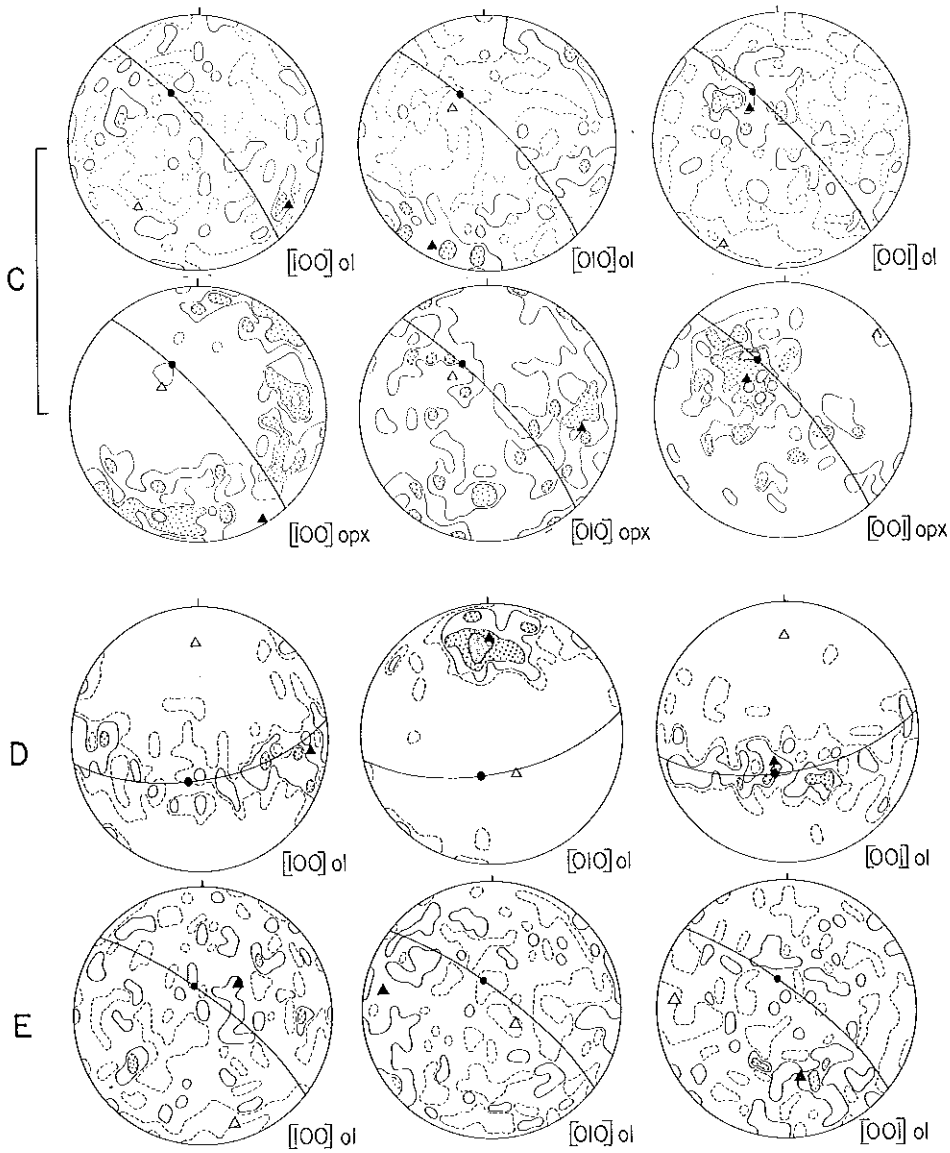


Fig. 8. Lower hemisphere equal area projection of crystallographic axes of olivine (ol) and orthopyroxene (opx). Geographical reference system: full line represents foliation; dot — lineation; triangles are computed point maxima (full) and pole of the best plan (open). Contours 0.5, 1, 2, 4% when 300 measurements, contours 1, 2, 4, 8% when 100 measurements, per 0.45% surface area.

A. Specimen CN 16 garnet peridotite from Lia body. Olivine: 300 measurements; orthopyroxene: 100 measurements.

B. Specimen CN 101 chlorite harzburgite from the shear zone near Lia body. Olivine: 300 measurements; orthopyroxene: 100 measurements.

C. Specimen CN 170 b chlorite dunite from the eastern fold. Olivine: 300 measurements; orthopyroxene: 100 measurements.

D. Specimen CN 221. Chlorite dunite from the western fold. Olivine: 100 measurements.

E. Specimen CN 2. Chlorite dunite from the eastern fold. Olivine: 100 measurements.

lization by rotation of subgrains (Poirier and Nicolas, 1975). This texture was produced in relatively dry conditions compared to the following ones, as shown by the scarcity of hydrous minerals (amphibole and chlorite).

*Mosaic tabular texture*

The reference type is characterized by a chlorite peridotite from the western body (Fig. 7D). Olivine crystals have a polygonal tabular shape; they define a clear foliation, also underlined by chlorite lamellae. The grain size varies from 0.3 to 2 mm; the grain-size distribution is very homogeneous throughout the section. Rare olivine grains exhibit widely spaced sub-boundaries. A strong crystallographic MPO (Fig. 8D) corresponds to the strong

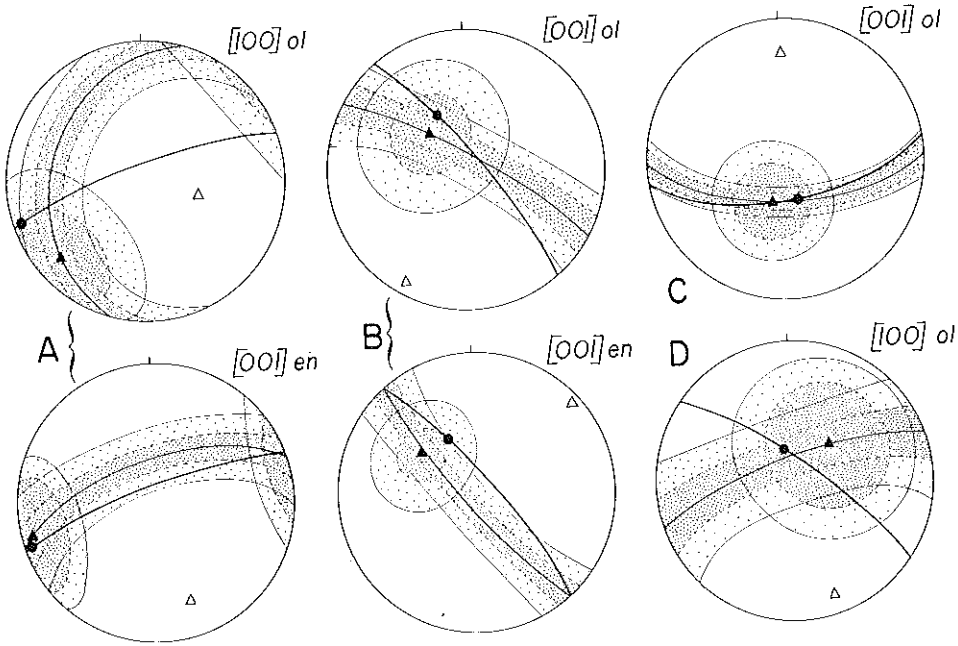


Fig. 9. Statistical point distribution calculated for fabric diagram of Fig. 8 which shows a maximum of preferred orientation close to the lineation. Cones and girdles centered respectively on the computed best axis and best plane contain 25% of the population (concentrated dots) and 50% of the population (diluted dots). Same reference system and conventions as in Fig. 8.

A. $\left.\begin{matrix}[100]_{ol}\\ [001]_{en}\end{matrix}\right\}$ in Fig. 8B, specimen CN 101.

B. $\left.\begin{matrix}[001]_{ol}\\ [001]_{en}\end{matrix}\right\}$ in Fig. 8C, specimen CN 170 b.

C. $[001]_{ol}$ in Fig. 8D, specimen CN 221.

D. $[100]_{ol}$ in Fig. 8E, specimen CN 2.

shape MPO (Fig. 7D). This MPO, characterized by a $[010]_{ol}$ maximum slightly oblique to the pole of the foliation and a girdle of $[100]_{ol}$ and $[001]_{ol}$ suggests the activation during the flow of two successive slip systems. The $[010]_{ol}$ orientation is consistent with the activation of the (010) $[100]_{ol}$ slip system ((010) close to the foliation), this fabric would be inherited from the high temperature $D_2$ deformation; the $[001]_{ol}$ orientation into subparallelism with $L_3$ is consistent with the activation of the $\{110\}$ $[001]_{ol}$ low temperature slip system related with the $D_3$ deformation. The complex fabric of Fig. 8D would result from superimposition of $D_2$ and $D_3$ deformations. The lack of reorientation of $\{110\}_{ol}$ plane into subparallelism with $S_3$ could be explained by competition between $(110)_{ol}$ and $(1\bar{1}0)_{ol}$ slip planes. The slight obliquity of the crystallographic MPO relative to the shape MPO (Fig. 9E) points to a shear flow regime (Nicolas et al., 1972).

Transitional types between (1) the mosaic equigranular and (2) the mosaic tabular textures occur in chlorite harzburgites from the eastern fold. Transition from (1) to (2) is marked by increasing grain-size and the acquisition of a tabular shape for olivine crystals (Fig. 7B, C), as the rock equilibrates in the chlorite-peridotite facies.

Two slightly different MPO's (Fig. 8B, C) illustrate these transitional textures. The first example is a chlorite peridotite from a shear zone adjacent to the garnet peridotite in the eastern body; the second is a chlorite harzburgite from the external part (100 m from the gneiss) of the eastern body. The enstatite shows a good $[001]_{en}$ maximum, close to the lineation and a $[100]_{en}$ girdle subperpendicular to the foliation, which is consistent with a process of deformation by intracrystalline slip (Nicolas et al., 1971) due to activation of the unique slip system of enstatite (100) $[001]_{en}$. Olivine shows diffuse maxima which appear only if the MPO is carried to 300 measurements. Different patterns are observed in the two examples. In the specimen from the inner shear zone (Fig. 8B) there is a tendency for a maximum of $[100]_{ol}$ slightly oblique to the lineation; in the specimen from the outer zone (Fig. 8C) this tendency exists for $[001]_{ol}$. In terms of intracrystalline slip, these patterns could be interpreted as due to the activation of the intermediate temperature slip system $\{Okl\}$ $[100]_{ol}$ in the first case and possibly the influence of the low temperature slip system $\{110\}$ $[001]_{ol}$ in the second. There is a small angle between foliation and lineation and computed best axes and poles of the best planes (Fig. 9B, C). This obliquity and the observed concordance between possible slip directions in olivine and the unique slip direction in enstatite both constitutes a good evidence for considering the development of the MPO's as resulting from intracrystalline slip by motion of dislocation (Nicolas and Poirier, 1976). Based on this interpretation, it is concluded that the lineations $L_1$, $L_2$ and $L_3$ (cf. Table I) are oriented at a small angle to the plastic flow direction which is marked by the maximum orientation of slip directions in enstatite and olivine (Fig. 8B, C). These observations are in accordance with the general case in peridotite. The weakness of the MPO's may be related to the fact that the strain was not

very large even taken into account the scattering effect of recrystallization (Nicolas and Poirier, 1976).

*Porphyroblastic textures* (Fig. 7E)

The porphyroblastic texture is representative of the chlorite-spinel dunites and the chlorite-spinel harzburgites of both peridotite bodies. It consists of relatively large (1—2 mm) polygonal olivine neoblasts surrounding large olivine porphyroblasts (10—50 mm). These large olivine crystals are considered to have developed by secondary enlargement since they always include chlorite lamellae. They have a wide-spaced ($\simeq$1 mm) sub-structure.

The olivine MPO in this textural type (Fig. 8E) appears to be random, though the computed best axis of the high temperatures slip direction $[100]_{ol}$ lies at a small angle to the spinel lineation (Fig. 9D). Post-tectonic recrystallization is considered to be responsible for the scattering of olivine orientations and for the secondary enlargement of porphyroblasts. The post-tectonic character of annealing is deduced from the low dislocation density observed in decorated sections (Ricoult and Gueguen, 1980).

*Role of water in the textural evolution*

The geographical distribution of the textural types related to their distance from surrounding gneisses, and the development of hydrous parageneses (amphiboles, chlorite, and finally antigorite) point to the role of water in the evolution of these textures. In this regard, the transition between garnet-peridotite cores and the adjacent shear zones is of special interest. There is precise correlation between the limit of shear zones, the chloritization of garnets and the development of an olivine MPO (Fig. 8A, B), possibly illustrating the influence of water in plastic flow and mineral reequilibration: in the garnet-peridotite cores, the absence of water prevented the plastic flow and preserved the texture and a metastable garnet in contrast with the shear zones. In the present study, stereograms of Fig. 8B indicate that the high temperature slip system would be operative in the shear zones in conditions fixed at 700° C and 10 kb. It is debatable whether water does not play a role in lowering the temperature limit of activation of olivine slip systems in wet peridotite, although experimentally there is no definitive evidence for or against the possibility of water-weakening in olivine (Paterson, 1979; Gueguen and Nicolas, 1980).

Finally, the role of water seems to be determinant in the development of strongly annealed textures characteristic of crustal peridotites with locally exaggerated grain growth (secondary annealing). This is illustrated in comparing the neoblast size in "dry" garnet peridotite and in adjacent "wet" chloritized peridotite (Fig. 7A, B); it is also illustrated by the development of large olivine porphyroblasts in the peridotite close to the contact with gneisses and especially along veins cross-cutting the recrystallized peridotite and carrying hydrous phases.

## AGE OF THE DEFORMATIONS

The Svecofennian age (1600—1800 Ma) assigned to the almandine-amphibolite metamorphism would suggest the same age for the development of $S_3'$ foliation in the gneisses and consequently a contemporaneous age for the deformations considered in this paper. Close to the peridotite—gneiss contact, eclogitic rocks occur which are restricted to Precambrian basement in the basal gneiss complex (Carswell, 1973).

This eclogite is partially retromorphosed in the almandine-amphibolite facies and flattened into the $S_3'/S_4$ foliations. It seems to have been emplaced in the same way as peridotite and perhaps at the same time (Jacobsen, 1980). It is therefore suggested that the Almklovdalen peridotite records the deformations which accompanied its emplacement from the mantle into the lower crust, probably during the Svecofennian orogenic cycle. The deformation was continuous, starting in the upper mantle with the dry garnet peridotite and evolving in a crustal environment responsible for the development of hydrous parageneses, progressing from the margins towards the core of the peridotite mass. The cycle of deformations was terminated with the development of a foliation in the gneiss. This phase was probably also responsible for the scattering of ultrabasic lenses in the gneiss as suggested by the geographical distribution of peridotite bodies in Nordfjord area, which follows the E—W to NE—SW orientation of the foliation in the gneisses (Bryhni, 1966).

In the Almklovdalen peridotite the Caledonian orogeny may be responsible for brittle deformation which indiced local recrystallization of olivine in a hydrated environment. From $^{86}Sr/^{87}Sr$ ratios on Almklovdalen garnet-peridotite, chlorite-peridotite on the one hand and fracture assemblages (olivine + tremolite + chlorite + phlogopite + talc) on the other, Brueckner (1975) indicated that only the fractured peridotites yield Caledonian ages.

## MODEL OF EMPLACEMENT

Gravity studies by Grønlie and Rost (1974) suggest that the Almklovdalen massif has a synform shape with the Helgehornet gneisses occupying the central part of the synform. They also suggest that the peridotite underlies the gneiss towards the southeast and extends several kilometers in that direction (Fig. 1). Synforms of amphibolite bodies included in more silica-rich formations have been described in the Nagu syncline, southwest Finland, by Metzger (1945) and interpreted by Lauren (1973), on the basis of a gravity map, as due to sinking of a dense amphibolite horizon during deformation of a surrounding granitic gneiss. Such an interpretation is proposed for the Almklovdalen peridotite body, based on: (1) the density differences between the peridotite ($d$ = 3.30) and the enclosing gneiss ($d$ = 2.65—2.72), (2) the shape of the structure revealed by geological and gravity studies (Figs. 1 and 6), and (3) the kinematic path of the deformation during the retrograde meta-

morphism which has been analyzed in this paper.

There is a striking consistency between the gravity map (Fig. 1) showing deep extension of the high density body towards the southeast, and the southeastward plunge of the large-scale fold axes and associated $L_3$, $L'_3$, $L_4$ lineations (p. 266). Moreover, the large-scale fold axes and the deformed $S_3$ foliations are steeper in the eastern fold than in the western fold (Fig. 5E—H). The gravity and structural data therefore suggest for the Almklovdalen body a cone-shaped structure with its apex rooted to the southeast as presented in Fig. 10A. The $S_3$ foliation would parallel the contours of the cone, and the $L_3$ lineation would parallel the generatrix of the cone. A possible reconstruction of the kinematic path followed by the Almklovdalen body is presented in Fig. 10. Figure 10A represents the present hypothetical shape

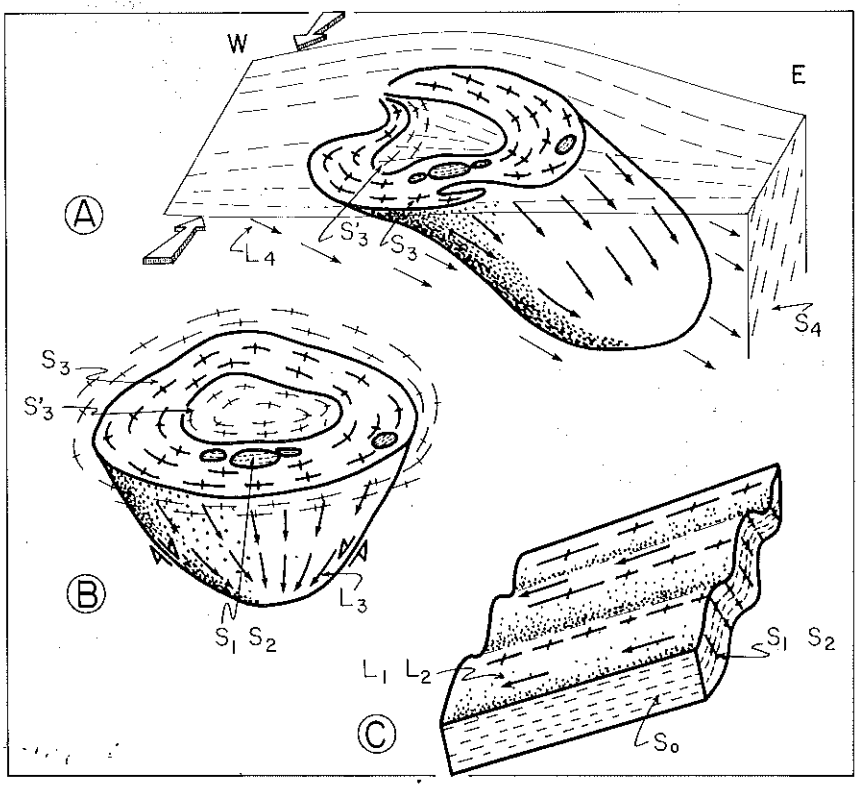


Fig. 10. Model of the emplacement of the Almklovdalen body. A.Present-day structure after the N—S flattening related to phase $D_4$, which is contemporary with retrograde metamorphism of the gneiss in low amphibolite facies. B. Development of the cone-shape structure by gravity sinking during phase $D_3$ contemporary with the equilibrium in crustal conditions (chlorite-peridotite facies in the ultramafites and almandine-amphibolite facies in the gneiss). C. Initial slice of mantle garnet-peridotite folded in conditions of garnet-peridotite facies during phase $D_1$ and in conditions transitional from garnet-peridotite to chlorite-peridotite facies during phase $D_2$.

of the structure. Flattening perpendicular to $S_4$ foliation in the surrounding gneiss would be responsible for deformation of the cone into two nested folds, this deformation occurred during amphibolite retrograde metamorphism of the gneiss (phase $D_4$). Figure 10B represents the sinking episode responsible for the cone-shape development and for the vertical foliations $S_3$ and $S_3'$ and the steeply plunging $L_3$ and $L_3'$ stretching lineations. This deformation was accompanied by shearing and occurred in the chlorite-peridotite equilibrium conditions for the peridotite and in the almandine-amphibolite facies for the gneiss. During this stage the peridotite was deformed plastically at 650—850° C in hydrated conditions. Olivine MPO indicates that the deformation operated by intracrystalline gliding following directions close to the $L_3$ stretching lineation (p. 275). It is hypothesized that the original structure was a flat slice of banded garnet peridotite, slightly dipping to the west and folded under garnet-peridotite facies conditions, with a fold axis slightly dipping to the west (Fig. 10C). Since the garnet is a primary phase, stable under mantle conditions (O'Hara et al., 1971), a mantle origin is proposed for the Almklovdalen garnet peridotite. From $^{143}Nd/^{144}Nd$ ratios, Jacobsen (1980) suggested that peridotites were emplaced during the formation of the crust in this region.

## CONCLUSIONS

Structural mapping and study of microstructure and mineral preferred orientations in the Almklovdalen peridotite massif lead to the following conclusions:

(1) Four phases of deformation are identified geometrically in the Almklovdalen structure. The three earlier phases are related to three textural types in peridotites whose distribution indicates decreasing $P$—$T$ condition from the core to the contact with gneiss. Relationships of parageneses and structural elements suggest that they represent a continuous path of deformation in retrograde $P$—$T$ conditions from mantle conditions in the garnet-peridotite facies through infracrustal and finally uppercrustal conditions of lower amphibolite facies. MPO's indicate that the peridotite first deformed plastically in dry garnet-peridotite conditions, then in hydrated chlorite-peridotite ones, and that foliations and stretching lineations are respectively close to the plastic flow planes and directions as deduced from the maxima of olivine and orthopyroxene crystallographic orientations. The three slip systems: the high temperature (010) $[100]_{ol}$, the $\{0kl\}$ $[100]_{ol}$ and possibly the low temperature $\{110\}$ $[001]_{ol}$ have been observed in olivine from chlorite peridotites. Annealed textures, despite the relatively low temperature of deformation emphasizes the role of water, which also has possible effects in lowering the temperature of activation of slip systems in olivine.

(2) Incorporating the gravity data in the structural and kinematic history suggests that the Almklovdalen body has a deformed synform cone shape which could result from gravity sinking of a slice of heavier peridotite in an

enclosing lighter and more ductile granitic gneiss. This cone-shaped structure was later deformed with the gneiss during a N—S compressional phase.

(3) Based on the Svecofennian age (1400—1700 Ma) of the almandine-amphibolite metamorphism in the gneiss, it is suggested that the emplacement and the sinking of the peridotite body occurred during or before Svecofennian time and that later events had minor effects on the Almklovdalen body.

ACKNOWLEDGMENTS

The authors are pleased to acknowledge A. Nicolas for fruitful suggestions and a constructive review of the paper. Financial support was obtained from RCP "Norvège" of the Centre National de la Recherche Scientifique.

REFERENCES

Boudier, F., 1976. Le massif lherzolitique de Lanzo (Alpes piémontaises). Etude structurale et pétrologique. Thèse Univ., Nantes, 163 pp.

Boullier, A.M. and Nicolas, A., 1975. Classification of textures and fabrics of South Africa peridotite xenoliths from kimberlite. Phys. Chem. Earth, 9: 467—476.

Brueckner, H.K., 1972. Interpretation of Rb-Sr ages from Precambrian and Paleozoic rocks of southern Norway. Am. J. Sci., 272: 334—358.

Brueckner, H.K., 1975. Contact and fracture ultramafic assemblages from Norway: Rb-Sr evidence for crustal contamination. Contrib. Mineral. Petrol., 49: 39—48.

Bryhni, I., 1966. Reconnaissance studies of gneisses, ultrabasites, eclogites and anorthosites in outer Nordfjord, western Norway. Nor. Geol. Unders. 241: 68 pp.

Bryhni, I., Green, D.H., Heier, K.S. and Fyfe, W.S., 1970. On the occurrence of eclogite in western Norway. Contrib. Mineral. Petrol., 26: 12—19.

Calon, T.J., 1973. De geologie van het Kittelfjäll. Daunatjakkogebied. Intern. Rep. Geol. Inst., Leiden.

Carswell, D.A., 1968. Possible primary upper mantle peridotite in Norwegian basal gneiss. Lithos, 1: 322—355.

Carswell, D.A., 1973. The age and status of the basal gneiss complex of northwest southern Norway. Nor. Geol. Tidsskr., 53: 65—78.

Carswell, D.A. and Gibb, F.G.F., 1980. The equilibration conditions and petrogenesis of european crustal garnet lherzolites. Lithos, 13: 19—29.

Carter, N.L. and Avé Lallemant, H.C., 1970. High temperature flow of dunite and peridotite. Geol. Soc. Am. Bull., 81: 2180—2202.

Gueguen, Y. and Nicolas, A., 1980. Mantle rocks deformation. Annu. Rev. Earth Planet. Sci., 8: 119—144.

Grønlie, G. and Rost, F., 1974. Gravity investigation and geological interpretation of the ultramafic complex of Åheim, Sunnmøre, western Norway. Nor. Geol. Tidsskr., 54: 367—373.

Jacobsen, S.B., 1980. Nd and Sr isotopes of the Norwegian garnet peridotites and eclogites. Am. Geophys. Union Spring Meet., 1980, Div. Contrib., 3420 (344).

Lappin, M.A., 1966. The field relationships of basic and ultrabasic masses in the Basal gneiss complex of Stadlandet and Almklovdalen, Nordfjord, southwestern Norway. Nor. Geol. Tidsskr., 46: 439—496.

Lappin, M.A., 1967. Structural and petrofabric studies of dunites of Almklovdalen, Nordfjord, Norway. In: P.J. Wyllie (Editor), Ultramafic and Related Rocks. Wiley, New York, pp. 183—190.

Lappin, M.A., 1973. An unusual clinopyroxene with complex lamellar intergrowths from an eclogite in the Sunndal-Grubse ultramafic mass. Almklovdalen, Norfjord, Norway. Mineralogy, 39: 313—320.

Lappin, M.A., 1974. Eclogites from the Sunndal-Grubse ultramafic mass. Almklovdalen, Norway and the T.P. history of the Almklovdalen masses. J. Petrol., 15: 567—601.

Lauren, L., 1973. Gravity study of the amphibolite syncline in Nagu SW-Finland. Bull. Geol. Soc. Finl., 45: 53—60.

Mc Dougall, I. and Green, D.H., 1964. Encess radiogenic argon and isotopic ages on mineral from Norwegian eclogites. Nor. Geol. Tidsskr., 40: 289—296.

Medaris, L.G., 1980. Convergent metamorphism of eclogite and garnet-bearing ultramafic rocks at Lien, West Norway. Nature, 283: 470—472.

Metzger, A.T., 1945. Zur Geologie der Inseln Ålö und Kyrklandet in Pargas-Parainen, S.W. Finnland. Acta Acad. Abo., Ser. B., 15: 3.

Möckel, J.R., 1969. Structural Petrology of the garnet peridotite of Alpe Arami (Ticino, Switzerland). Leidse Geol. Meded., 42: 61—130.

Mysen, B.O. and Heier, K.S., 1972. Petrogenesis of eclogites in high grade metamorphic gneisses exemplified by the Hereidland Eclogite, western Norway. Contrib. Mineral. Petrol., 36: 73—99.

Nicolas, A. and Boudier, F., 1975. Kinematic interpretation of folds in alpine type peridotites. Tectonophysics, 25: 233—260.

Nicolas, A., Bouchez, J.L., Boudier, F. and Mercier, J.C., 1971. Textures, structures and fabrics due to solid state flow in some European lherzolites. Tectonophysics, 12: 55—58.

Nicolas, A., Boudier, F. and Boullier, A.M., 1972. Mechanisms of flow in naturally and experimentally deformed peridotites. Am. J. Sci., 273: 853—876.

Nicolas, A. and Poirier, J.P., 1976. Crystalline Plasticity and Flow in Metamorphic Rocks. Wiley, London.

O'Hara, M.F. and Mercy, E.L.P., 1963. Petrology and petrogenesis of some garnetiferous peridotites. Trans. R. Soc. Edinb., 65: 251—314.

O'Hara, M.J., Richardson, S.W. and Wilson, C.R., 1971. Garnet peridotite stability and occurrence in crust and mantle. Contrib. Mineral. Petrol., 32: 48—68.

Paterson, M.S., 1979. The mechanical behaviour of rocks under crustal and mantle conditions. In: M.W. McElhinny (Editor), The Earth, its Origin, Structure and Evolution. Academic Press, London, pp. 469—489.

Pidgeon, R.T. and Raheim, A., 1972. A geochronological investigation of the gneisses and minor intrusive rocks from Kristiansund, West Norway. Nor. Geol. Tidsskr., 52: 241—256.

Poirier, J.P. and Nicolas, A., 1975. Deformation-induced recrystallisation by progressive misorientation of subgrain-boundaries, with special reference to mantle peridotites. J. Geol., 83: 707—720.

Ricoult, D. and Gueguen, Y., 1980. Experimental studies on the recovery process of deformed olivines and the mechanical state of the upper mantle. Discussion. Tectonophysics, 65: 181—192.

Rost, F., 1963. Ultrabasite der Kruste und ihr Mineralbestand. Neues Jahrb. Mineral. Monatsh., 1963: 263—272.

Rost, F., 1971. Probleme der Ultramafitite. Fortschr. Mineral., 48: 54—68.

Rost, F., Wannemacher, J. and Grigel, W., 1974. Die Ultramafitite der Alpe Arami und Croveggio, Tessin. Schweiz. Mineral. Petrogr. Mitt., 54: 353—369.

Tromsdorff, V. and Evans, B.W., 1974. Alpine metamorphism of peridotite rocks. Schweiz. Mineral. Petrogr. Mitt., 54: 333—352.

Weiss, L.E., 1977. Structural features of the Zakevåg gneiss, Laksevåg, Bergen. Nor. Geol. Unders., 334: 1—17.